European Journal of Cell Biology 89 (2010) 757–768

Contents lists available at ScienceDirect

European Journal of Cell Biology

journal homepage: www.elsevier.de/ejcb

Differential relocation and stability of PML-body components during productive human cytomegalovirus infection: Detailed characterization by live-cell imaging

Panagiota Dimitropoulou[a], Richard Caswell[b], Brian P. McSharry[c], Richard F. Greaves[d], Demetrios A. Spandidos[a], Gavin W.G. Wilkinson[c], George Sourvinos[a,*]

[a] Department of Virology, Faculty of Medicine, University of Crete, Heraklion 71003, Crete, Greece
[b] Cardiff School of Biosciences, Cardiff University, Cardiff, Wales, United Kingdom
[c] Department of Infection, Immunity and Biochemistry, Tenovus Building, Cardiff University, Heath Park, Cardiff CF14 4XN, United Kingdom
[d] Department of Virology, Division of Investigative Science, Imperial College Faculty of Medicine, St Mary's Campus, Norfolk Place, London W2 1PG, United Kingdom

ARTICLE INFO

Article history:
Received 5 March 2010
Received in revised form 14 May 2010
Accepted 26 May 2010

Keywords:
HCMV
IE1-72K
ND10
PML
Sp100
hDaxx
STAT1
STAT2
Condensed chromatin
Live-cell microscopy

ABSTRACT

In controlling the switch from latency to lytic infection, the immediate early (IE) genes lie at the core of herpesvirus pathogenesis. To image the 72 kDa human cytomegalovirus (HCMV) major IE protein (IE1-72K), a recombinant virus encoding IE1 fused with EGFP was constructed. Using this construct, the IE1-EGFP fusion was detected at ND10 (PML-bodies) within 2 h post infection (p.i.) and the complete disruption of ND10 imaged through to 6 h p.i. HCMV genomes and IE2-86K protein could be detected adjacent to the slowly degrading IE1-72K/ND10 foci. IE1-72K associates with metaphase chromatin, recruiting both PML and STAT2. hDaxx, STAT1 and IE2-86K did not re-locate to metaphase chromatin; the fate of hDaxx is particularly important as this protein contributes to an intrinsic barrier to HCMV infection. While IE1-72K participates in a complex with chromatin, PML, STAT2 and Sp100, IE1-72K releases hDaxx from ND10 yet does not appear to remain associated with it.

Introduction

Human cytomegalovirus (HCMV) is the prototype member of the *Betaherpesvirinae* (family *Herpesviridae*), the major viral cause of congenital malformation and is associated with a wide range of clinical disease, particularly in immunocompromised individuals. However, HCMV is a ubiquitous virus and the vast majority of infections are well tolerated. As with other herpesviruses, primary infection is followed by lifelong persistence that must be continuously restrained by host immune surveillance. Myeloid progenitor cells appear to be the primary site of latency/persistence, with virus reactivation being associated with differentiation into macrophages or dendritic cells. *In vivo*, virus replication can be detected in a wide range of cell types (Sinzger et al., 1995).

By definition, the immediate early (IE) genes are expressed first and are responsible for activating the transcription of HCMV early genes. IE2-86K encodes a powerful, promiscuous transcriptional trans-activator that plays the major role in advancing the transcriptional cascade (Marchini et al., 2001; Pizzorno et al., 1988). To establish an environment compatible with efficient virus replication, IE gene expression acts to counter intrinsic, innate and adaptive host immune defenses. UL36 and UL37 inhibit apoptosis (Goldmacher et al., 1999; Skaletskaya et al., 2001), IRS1/TRS1 suppress the interferon response (Child et al., 2004) while US3 downregulates cell surface expression of MHC class I gene expression (Ahn et al., 1996). While the 72 kDa major IE protein (encoded by *IE1*) is not essential for virus replication *in vitro*, an IE1 (exon 4) deletion mutant exhibits a growth defect at low multiplicity of infection (Greaves and Mocarski, 1998; Mocarski et al., 1996). The HCMV IE1-72K has pleiotropic functions, it upregulates its own promoter (Cherrington and Mocarski, 1989), enhances transcriptional activation by IE2-86K (Malone et al., 1990), antagonizes histone deacetylation (Nevels et al., 2004; Reeves et al., 2006), is a kinase capable of autophosphorylation in addition to targeting E2F-1-3, p107 and p130 (Pajovic et al., 1997), promotes cell cycle progression (Castillo et al., 2000; Fortunato et al., 2002), suppression of the interferon response (Boyle et al., 1999; Browne et al., 2001; Navarro et al., 1998; Simmen et al., 2001; Zhu et al., 1997) and disruption of ND10 (Ahn et al., 1998; Ahn and Hayward, 1997; Kelly et al., 1995;

* Corresponding author.
E-mail address: sourvino@med.uoc.gr (G. Sourvinos).

0171-9335/$ – see front matter © 2010 Elsevier GmbH. All rights reserved.
doi:10.1016/j.ejcb.2010.05.006

Korioth et al., 1996; Wilkinson et al., 1998). ND10 are punctate intranuclear bodies associated with the tumour suppressor protein PML, and are also known as PML-bodies or PML oncogenic domains (PODS).

Herpesvirus genomes are deposited adjacent to ND10 immediately following infection, and this is the site at which virus transcription and DNA replication are initiated (Ahn et al., 1999; Everett et al., 2003; Ishov and Maul, 1996; Ishov et al., 1997; Maul et al., 1996; Sourvinos and Everett, 2002; Sourvinos et al., 2007). ND10 are dynamic intranuclear domains bound to the nuclear matrix, implicated in cellular transcription, chromatin structure, DNA repair, mitosis and apoptosis (Bernardi and Pandolfi, 2003; Dellaire and Bazett-Jones, 2004). While they are defined by the presence of PML, cellular proteins that have been associated with ND10 include: Sp100, hDaxx, SUMO-1, p53, STAT1, STAT2, ATRX (Choi et al., 2006; Ishov et al., 2004; Lukashchuk et al., 2008; Negorev and Maul, 2001; Paulus et al., 2006; Tang et al., 2004). Interestingly, PML is an interferon-inducible protein and many DNA viruses impact on the integrity of ND10. PML-bodies are now recognized to constitute an intrinsic barrier to virus infection. In this context, RNAi knockdown of either PML or hDaxx significantly enhanced HCMV or HSV-1 replication (Everett, 2006; Lukashchuk et al., 2008; Tavalai et al., 2006, 2008).

Besides its interaction with ND10, IE1-72K is also known to associate with condensed chromatin in HCMV-infected cells during mitosis (Ahn et al., 1998; Lafemina et al., 1989; Wilkinson et al., 1998). Exactly how the targeting and overt physical disruption of PML-bodies together with IE1's association with mitotic chromatin relate to its roles in promoting virus replication have yet to be determined. In this study, IE1-72K targeting and disruption of ND10 immediately following infection, together with the close association with both IE2-86K and the HCMV parental genomes were visualized in lytic infection. Live-cell imaging with an HCMV recombinant encoding an IE1-EGFP fusion protein clearly demonstrated IE1-72K associated with PML, Sp100 and STAT2 on metaphase chromatin, but not with hDaxx or STAT1. The dynamic and differential re-organization of ND10 components to cellular chromatin (PML, STAT2), degradation (Sp100) or release into the nucleoplasm (hDaxx) can be expected to relate mechanistically with IE1's functional role in regulating gene expression and preparing the cell for infection.

Materials and methods

Plasmids

For the construction of IE1 (exon 4)-EGFP fusion, the plasmid pON2512 (Gawn and Greaves, 2002) was initially used, containing a HCMV Towne strain DNA fragment from *Bgl*II site in exon 4 to *Sal*I site downstream of exon 5 of the *ie1*/*ie2* locus. Site-directed mutagenesis was carried out using the oligonucleotide 5′ TAT ATA CAA TAG **G**T**A** **C**CT GGT CAG CCT TGC 3′ (mutagenic bases in bold) to remove the stop codon of exon 4 and simultaneously introduce a unique *Kpn*I site, to generate the plasmid pON2512Kpn. In parallel, the EGFP coding sequence was excised from plasmid pEGFP-N1 (Clontech) after digestion with *Not*I restriction enzyme followed by treatment with Klenow fragment and further digestion of the vector with *Kpn*I. The pON2512Kpn was digested at the novel *Kpn*I site and at the *Bst*1 1071 site located between the end of exon 4 coding sequence and *ie*1 poly A signal, and subsequently was ligated in frame with EGFP fragment to form pON2512Kpn-GFP. The latter was digested with *BglII* and at the *Xba*I site located immediately downstream of *Sal*I site and cloned into the same sites of pG303. pG303 contains the entire MIEP region, and upstream ORFs UL127-UL130 from Towne, on a 7.4 kb *Sal*I fragment, generating pG303-EGFP. Subsequently, the entire *ie1*–*ie2* coding region was sequenced in this plasmid, showing that no unexpected mutations had been introduced either during the site-directed mutagenesis or subsequent sub-cloning steps.

Plasmid pEGFP-IE1 was generated after fusion of the *ie1* gene derived from the pGEX-3X-IE1 (Caswell et al., 1993) to the Clontech vector pEGFP–C2. The autofluorescent expression vector pHcRed1-H2A was constructed after PCR amplification of the H2A gene and its insertion into the *Eco*RV site of the pBlue-Script KS vector (Stratagene, La Jolla, CA). Subsequently, the *Xho*I-*Eco*RI fragment was excised and ligated into the same sites of the vector pHcRed1-N1/1 (Clontech) to create pHcRed1-H2A. For construction of a vector expressing IE1 fused to mRFP1, the IE1 coding sequence was amplified from pGEX-3X-IE1 by PCR using the primers: Forward 5′ AAGAGAATTCATGGAGTCCTCTGCCAAGAG 3′ and Reverse 5′ CCTTGAATTCTTACTGGTCAGCCTTGCTTC 3′, containing *Eco*RI restriction sites. The purified PCR product was subsequently cloned into the *Eco*RI site of the pRSET$_B$mRFP1 vector, expressing the monomeric red fluorescent protein, to produce pRSET$_B$mRFP1-IE1. STAT1 and STAT2 cDNAs were cloned in fusion with mCherry under the control the HCMV MIEP using recombineering technology as described (Stanton et al., 2008).

The expression vectors pEGFP-IE2 and pmCherrySp100 (Sourvinos et al., 2007) as well as pECFP-PML (Everett et al., 2003) have been described previously.

For transfection experiments, primary human foreskin fibroblasts (HFFs), mChSp100 cells or HeLa cells were seeded either on glass coverslips or into four-well, chambered coverglass units with coverslip quality glass bottoms (Lab-Tek; Nunc). For transient expression assays, DNA (1 μg/well) was introduced in subconfluent cells using the TransPEI transfection reagent (Eurogentec, Belgium) according to the manufacturer's instructions.

Cells and viruses

HFF and HeLa cells were maintained in Dulbecco's modified Eagle's medium (Biosera, UK) supplemented with 10% fetal calf serum. HFFs stably expressing the Sp100A isoform fused to the monomeric red autofluorescent protein mCherry were maintained as previously described (Sourvinos et al., 2007). HFFs with a stable small interfering RNA-mediated kd of PML were cultured in Dulbecco minimal essential medium supplemented with 10% fetal calf serum and 5 μg of puromycin/ml (kind gift of Thomas Stamminger, University Erlangen-Nürnberg, Germany (Tavalai et al., 2006)). The wild-type HCMV strain AD169 as well as HCMV AD169/IE2-EGFP (Sourvinos et al., 2007) was also employed.

Virus plaque assays were performed on HFFs according to standard protocols. To characterize the growth properties of the CR401 virus, single-step growth curves were performed in parallel with wt HCMV AD169 and the viral titres were determined via IE1 staining (Andreoni et al., 1989).

Bacterial artificial chromosome (BAC) generation and reconstitution of the HCMV BAC virus

BAC DNAs were propagated as previously described (Borst et al., 1999). The BAC plasmid pHB5 (Borst et al., 1999) was used for the construction of the CR401 virus, as follows. The *ie1*-exon 4 was removed from pHB5 after digestion with *Acc*I, generating an intermediate exon 4-deleted BAC. A *Bgl*II-*Xho*II fragment from pG303-EGFP, including EGFP sequences and flanking regions of *ie*1 and *ie*2 genes was sub-cloned between *BamH*I and *Sal*I sites of shuttle vector pKOV-KanF (Lalioti and Heath, 2001). Co-integrants between this vector and pHB5 BAC were isolated and then resolved in DH10B bacteria, according to the method of Lalioti and Heath (2001). The structure of the resultant recombinant BACs carrying

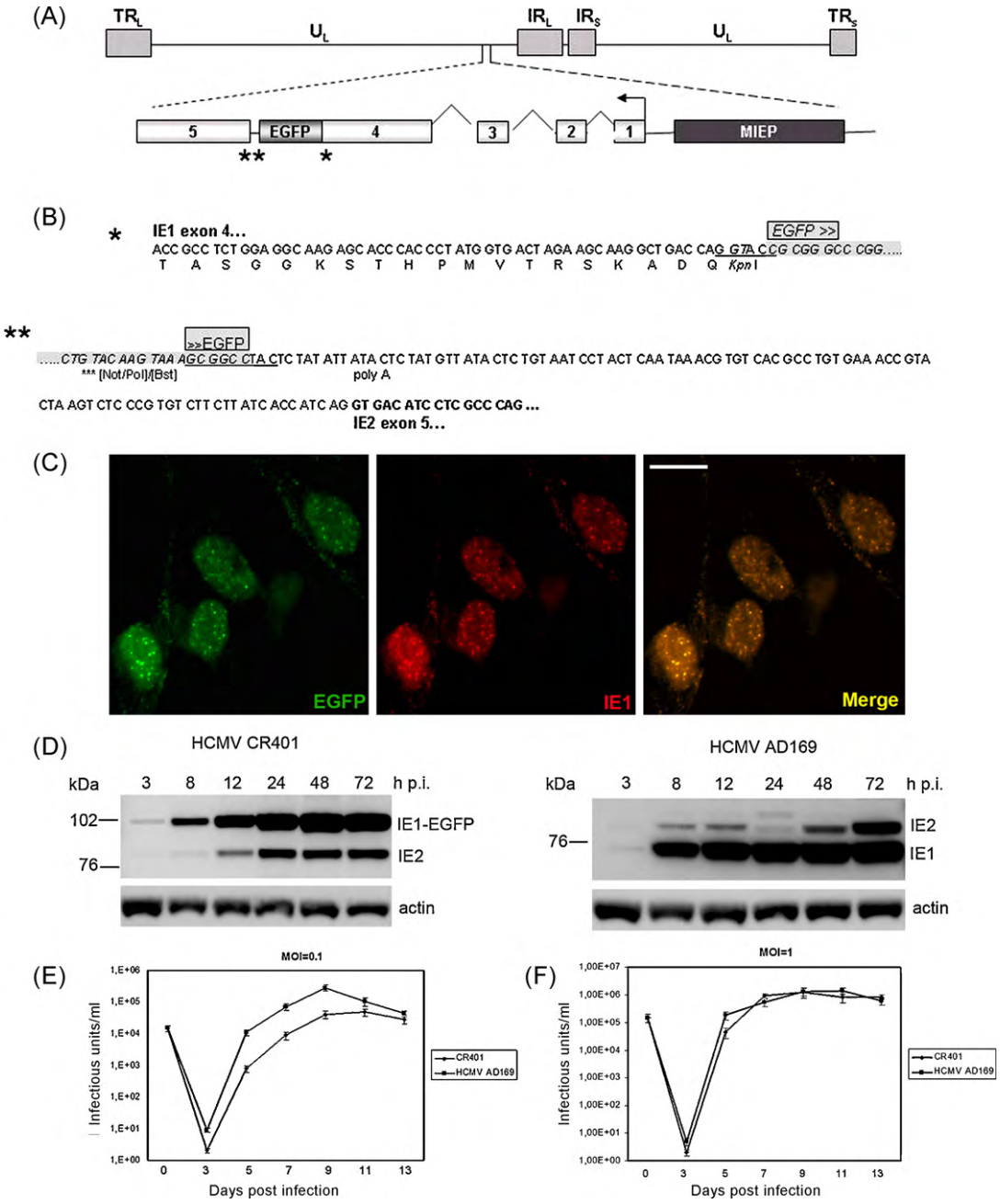

Fig. 1. Construction and characterization of the HCMV CR401 virus. (A) Schematic representation of the HCMV genome region in which the *ie1*-exon 4-EGFP coding sequence was inserted. (B) The asterisks show the sequences between *ie1*-exon 4 and the EGFP coding sequence as well as between EGFP ORF and *ie2*-exon 5. (C) Subcellular co-localization of IE1 (red) and EGFP (green) detected by indirect-immunofluorescence assays in CR401-infected HFF 3 h p.i. (D) Kinetics of IE viral antigen expression. Viral immediate-early antigen IE1-72K and IE2-86K were detected in both HCMV CR401 and wt HCMV AD169-infected HFF at MOI = 1 by Western blotting at the indicated time points. (E and F) HFF cells were infected in parallel at M.O.I. = 0.1 and M.O.I. = 1 with viral inocula of wt HCMV AD169 (filled rectangles) or CR401 (filled diamonds) which were standardized for equal IE1 expression at 24 h p.i. The virus progeny in the supernatants of infected cell cultures were harvested at different time points p.i. as indicated, followed by quantification of the viral load via IE1 fluorescence. Error bars indicate the standard deviation derived from three independent experiments (For interpretation of the references to color in this figure legend, the reader is referred to the web version of the article.).

the *ie*1-EGFP fusion were verified by FIGE, to yield BAC CR401 (Fig. 1 A and B). The recombinant CR401 virus was reconstituted as previously described (Reboredo et al., 2004).

Immunofluorescence and Western blot

The HCMV IE1 and IE2 gene products were detected using monoclonal antibodies against IE1-72K (BS500) and IE2-86K (SMX) as previously described (Plachter et al., 1993). For the detection of endogenous PML, Sp100, hDaxx, STAT1 and STAT2 the monoclonal antibodies PML (H-238), Sp100 (H-60), Daxx (M-112), STAT1 (H-95) and STAT2 (H-190) (rabbit polyclonal) from Santa Cruz Biotechnology (Santa Cruz, CA) were used, respectively. Sp100 was detected in Western blots using a rabbit polyclonal anti-SP100 antibody GH3 (kind gift of Hans Will, Heinrich-Pette Institute, Germany (Milovic-Holm et al., 2007)). The monoclonal antibody (MAb) Ac-15 which recognizes β-actin was purchased from Chemicon International, Inc. Anti-mouse as well as anti-rabbit horseradish peroxidase-conjugated secondary antibodies were obtained from Sigma while Alexa 488-, Alexa 555- and Cy3-conjugated secondary antibodies were purchased from Molecular Probes.

For indirect-immunofluorescence analysis, primary HFF cells (1×10^5) were grown on coverslips for transient transfection or HCMV infection, respectively. The conditions for transfection of HFFs, as well as for fixation and immunodetection of viral and cellular proteins, were as previously described (Everett et al., 2003).

For Western blotting, extracts from infected cells were prepared in sodium dodecyl sulfate loading buffer, separated on sodium dodecyl sulfate-containing 8–15% polyacrylamide gels, and transferred to nitrocellulose membranes. Western blotting and chemiluminescence detection were performed as previously described (Everett et al., 2003).

Fluorescence in situ hybridization

Fluorescence *in situ* hybridization was performed according to a previously described protocol (Everett and Murray, 2005) with appropriate modifications for HCMV (Sourvinos et al., 2007). HFF cells were grown on 13-mm diameter glass coverslips and then infected with HCMV AD169 either at a multiplicity of infection of 0.1 PFU/cell or 1 PFU/cell.

Time-lapse microscopy of live cells

Cells were seeded into four-well, chambered coverglass units with coverslip quality glass bottoms (Lab-Tek; Nunc) at a density of 1×10^5 cells per well the day before each experiment. Live cells were observed using the ×63 dry objective lens of a Leica DMIRE2 inverted fluorescence microscope equipped with a Leica DFC300 FX digital camera. The microscope stage was enclosed within a controlled environment of constant temperature, CO_2 and humidity in order to maintain cell viability during experiments. Excitation wavelength was controlled by mercury lamp illumination and a manual filter wheel equipped with filters suitable for EGFP, the monomeric red fluorescent protein mCherry and DAPI. The camera image acquisition was controlled by the IM50 software (Leica). Special care was taken in order to avoid overlap between channels by collecting the data from each channel sequentially and routing the emission signals through appropriate band pass filters. Single images or timed image sequences were exported as TIFF files from the IM50 software.

Results

Characterization of HCMV CR401

In order to visualize the IE1-72K protein directly during infection, the recombinant HCMV CR401 was generated by in-frame insertion of EGFP at the C-terminus of IE1 (Fig. 1A and B). In HCMV CR401-infected cells (3 h p.i.), IE1-GFP protein exhibited a diffuse nuclear distribution with focal concentrations at ND10 (Fig. 1C), similar to the staining pattern observed with IE1-72K in the parental virus (Kelly et al., 1995). Furthermore, staining with an IE1-specific antibody co-localized with EGFP fluorescence (Fig. 1C). Additionally, the EGFP-IE1 signal precisely co-localized with IE1-72K in cells infected with wild-type HCMV and co-transected with pEGFP-IE1 (Fig. S1). The reduced relative mobility of IE1-GFP (100 kDa) to IE1 (72 kDa) was consistent with the predicted size increase associated with GFP fusion. The fusion protein was not only stable, but produced with similar kinetics and abundance to unmodified IE1 (Fig. 1D).

To characterize HCMV CR401, its growth properties were compared with strain AD169. At an M.O.I. of one, the growth kinetics of HCMV CR401 was identical to that of the parental virus. However, HCMV CR401 exhibited delayed kinetics and reduced peak yield virus at an M.O.I. of 0.1 (Fig. 1E and F). IE1-72K and IE2-86K are derived by differential splicing from the same transcriptional unit, IE1-72K being encoded by exons 1, 2, 3, and 4 while the predominant IE2-86K transcript comprises exons 1, 2, 3 and 5. Expression of the predominant 86 kDa IE2 gene product was not overtly impaired by insertion of GFP insertion at this locus (Fig. 1D). By generating an HCMV recombinant encoding IE1-72K from its orthotopic position with a C-terminal GFP fusion, it becomes possible to image the major IE1-72K protein and its interaction with cellular proteins in the context of a productive infection.

Induction of PML dispersal and desumoylation by HCMV CR401

HCMV CR401 permits live-cell imaging of IE1-72K during infection, provides enhanced sensitivity of detection while eliminating potential artefacts associated with sample fixation and preparation. With HCMV CR401, IE1-EGFP was readily detected as early as 2 h p.i. and was predominantly associated with ND10, interspersed with diffuse staining in the majority of infected cells (Fig. S2A fixed cells, Fig. 2A a live-cell imaging). As the infection progressed PML was displaced from ND10, so that by 6 h p.i. endogenous PML was completely dispersed throughout the nucleoplasm in cells expressing IE1-EGFP (Fig. S2A (d–f)). While PML remains stable throughout infection, HCMV alters the extent of PML modification by SUMO adducts (Lee et al., 2004; Muller and Dejean, 1999). Sumoylation of PML at multiple sites produces a series of slower migrating forms of the protein (mock sample; Fig. S2B). IE1-72K is responsible for loss of sumoylated forms of PML during HCMV infections (Muller and Dejean, 1999) and this property was clearly retained by IE1-GFP in HCMV CR401 (Fig. S2B).

The rate of the IE1-72K redistribution to and from punctate foci was comparable at different M.O.I.s (data not shown). However, the number of IE1-72K foci was dependent on the multiplicity of the infection (compare Fig. 2A, a and c). Cells were analyzed from a large number of random fields captured 3 h p.i.; the average number of IE1-72K foci at M.O.I. = 1 was approximately three-fold higher (19 ± 4) than that at M.O.I. = 0.1 (7 ± 2). The finding that the amount of formation of IE1-72K foci is proportional to the M.O.I. suggests that viral or virally induced host factors might contribute to their formation.

Imaging Sp100 as ND10 disperse in HCMV infection

Studies in fixed cells have shown that IE1-72K traffics to ND10 and causes cellular PML to be displaced, with both proteins redistributing to a nuclear-diffuse pattern (Ahn et al., 1998; Ahn and Hayward, 1997; Korioth et al., 1996; Wilkinson et al., 1998). By utilizing the EGFP tag in HCMV CR401, the dynamic interaction between IE1-72K and ND10 can be imaged in live, infected cells. Primary human fibroblasts stably expressing the ND10 protein Sp100 (isoform A) fused with a red (mCherry) fluorescent protein (mChSp100) were infected with CR401 and the localization of HCMV *ie1* gene product and of the cellular Sp100 was analyzed by time-lapse microscopy. Fig. 2B presents a sequence of images of an individual live, infected cell during the course of the infection. The vast majority of IE1-EGFP co-localized with Sp100 in ND10 at 200 min p.i. and IE1 and Sp100 remained in close association, with minimal movement, throughout the sequence. Over time, IE1-EGFP changed from a focal to a nuclear-diffuse distribution as ND10 disintegrated. Remarkably, with the disruption of ND10 and in contrast to the diffuse distribution of PML in the nucleus, the mChSp100 signal progressively faded in the nucleus. The rate of Sp100 elimination was comparable at different M.O.I.s as time-lapse experiments demonstrated. Given that Sp100 is a low-abundance protein (Negorev et al., 2006), we sought to investigate biochemically the effect of IE1-EGFP on Sp100 at early stages of the infection by Western blot in fibroblasts overexpressing the Sp100 protein fused to mCherry. As shown in Fig. 2C, HCMV CR401

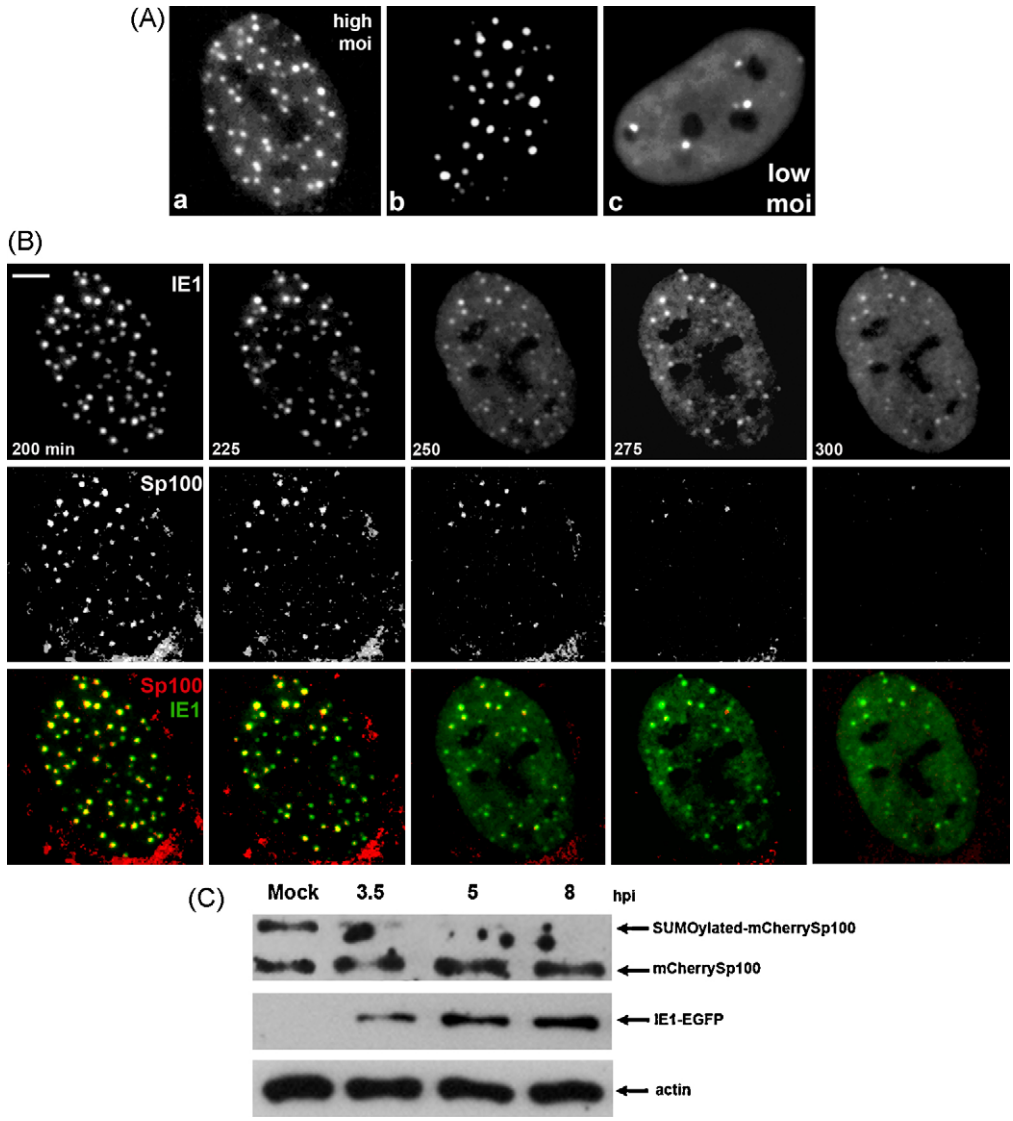

Fig. 2. Dynamic nuclear redistribution of IE1 and imaging of Sp100 as ND10 disperse in live-infected cells. (A) HFF cells were infected with CR401 at M.O.I. = 1 and images were obtained by live-cell microscopy. IE1 displayed punctate foci, interspersed with a diffuse pattern in the nucleus (a), while in a proportion of infected cells IE1 was exclusively distributed in discrete intense dot-like structures (b) at 2 h p.i. The number of IE1 foci differed when cells were infected at M.O.I. = 0.1 (compare a and c). (B) Live human fibroblasts expressing mCherrySp100, infected with CR401 at M.O.I. = 1 were monitored at immediate early times after infection. The initially formed IE1 foci were dispersed during the course of a productive infection (200–300 min). Presented are selected double-labelled images that illustrate the dynamic dispersal of Sp100 by IE1 (bars, 10 μm). (C) mCherrySp100 cells were infected with HCMV CR401 at MOI = 1 or were mock infected; cells were harvested at the indicated time points after virus adsorption and total cell proteins were analyzed by Western blotting.

infection resulted in the progressive abolishment the SUMO-1 modification of Sp100 and by 8 h p.i. the SUMO-1-Sp100 conjugate was barely detectable. The results from both time-lapse and biochemical analysis provide solid evidence regarding the fate of Sp100 during HCMV infection, showing that the SUMO-1 modified isoform of Sp100 is predominantly dispersed from ND10 in an IE1-72K-dependent-manner.

Rapid elimination of ND10 takes place only in the context of viral infection

IE1-72K alone is sufficient to cause disruption of ND10. A plasmid encoding the EGFP-IE1 fusion protein (pEGFP-IE1) was transfected in mChSp100 cells and images were acquired over time. During infections with HCMV CR401, efficient IE1-EGFP expression and degradation of the mChSp100 signal was observed by 6 h p.i. (Fig. S3A, row A). With DNA transfection, the IE1-EGFP signal was first detected after 9 h, at which time mChSp100 could readily be detected in foci co-localized with IE1 (Fig. S3A, row B). The numbers of IE1 and Sp100 foci diminished progressively over time (Fig. S3A, rows C and D), and eventually disappeared (not shown). Within an individual cell, even after the majority of ND10 had been dispersed a number could be observed to persist (see arrows in Fig. S3A, row B), indicating a subset of ND10 were more resilient.

Subsequently, we quantified the association between IE1-72K and Sp100 by time-course analysis both after DNA transfection and CR401 infection of mChSp100 cells. In transfected cells, there was almost equal distribution at 9 h post-transfection of cells displaying either focal co-localization of IE1 and Sp100 and those showing punctate distribution of IE1 but with simultaneous dispersal of Sp100. Over the following 6 h, this pattern changed such that the majority of cells showed diffuse IE1 localization along with loss of Sp100 signal (Fig. S3Bi). Interestingly, in a few cells Sp100 foci remained intact until later times. In contrast, during productive infection with CR401 at two M.O.I.s, a similar pattern of redistribution of IE1 and Sp100 took place but over significantly shorter

periods (Fig. S3Bii and Fig. S3Biii). Thus, the mode of expression of IE1-72K has consequences for the subsequent effects of the protein in modifying the sub-nuclear environment. This time course is consistent with the HCMV major IE promoter (MIEP) being stimulated by virion components when delivered by the virus. Yet additional *de novo* HCMV-encoded functions could also influence events.

Subcellular localization of IE1-72K and HCMV parental genomes

Fluorescent *in situ* hybridization was employed to detect HCMV genomic DNA within infected cells. Early during infection, nearly all HCMV CR401 viral DNA labelling was associated with IE1 foci (Fig. 3A, rows A and B). Viral DNA and IE1 foci did not precisely co-localize, but were juxtaposed or partially overlapped. Considering that at similar time points of infection, HCMV transcripts emanating from ND10-associated genomes have also been detected (Ishov et al., 1997; Maul and Negorev, 2008), we might assume that the low proportion of non-IE1-72K-associated genomes are transcriptionally inactive. A similar pattern was observed for HCMV DNA and PML (Fig. 3A, row C). There were clearly many more IE1 foci than HCMV genomes, although the ratio closed at increasing M.O.I.

Differential localization of IE1-72K and IE2-86K in live-infected cells

IE1-72K and IE2-86K act together as the central regulators of the viral transcriptional cascade and to modulate cellular gene expression. Immediately following infection IE1-72K co-localizes with ND10, IE2-86K traffics to ND10 but is found in juxtaposition rather than precisely co-localized. In HCMV CR401-infected cells, this juxtaposition was readily apparent when IE2-86K expression was detected by immunofluorescence (Fig. 5B). The relationship between ND10 and IE2-86K is dynamic (Sourvinos et al., 2007). We sought to image IE1-72K and IE2-86K simultaneously in productive infection. HFFs were first transfected with a plasmid encoding mRFP1-IE1 and subsequently infected with HCMV AD169/IE2-EGFP (M.O.I. = 1). Cells were followed from when IE2-86K was first detected (2 h p.i.; Fig. 3C). A majority of IE1 and IE2 foci were distinguishable, yet in close association. Interestingly, during the course of the infection, the punctate foci of the two proteins constantly changed relative positions. Detailed analysis at high magnification revealed a dynamic relationship, with IE1-72K and IE2-86K in juxtaposition for most of the infection but some of them rapidly fused to precise co-localizations for a limited period, followed by their segregation. These data are consistent with IE1-72K co-localizing with ND10 while IE2-86K molecules form distinct foci, corresponding to separate discrete structures that frequently associate with ND10-IE1 accumulations early after infection.

Recruitment of IE1-72K onto metaphase chromatin in live cells

In fixed cells, HCMV IE1-72K protein can be detected tethered to mitotic chromosomes either when expressed in isolation or by HCMV infection (Ahn et al., 1998; Lafemina et al., 1989; Wilkinson et al., 1998). When HCMV CR401-infected cultures were examined, IE1-EGFP labelled condensed chromatin of all infected cells in mitosis (Fig. 4A) and was observed to co-localize with histone H2A (Fig. 4B), beginning at about 12 h p.i. However, when followed by live-cell imaging, these cells failed to progress out of metaphase through cell division, not allowing HCMV to spread in infected cells by cell division with continued expression of the major transactivating viral proteins. Therefore, the blockade of these cells on mitosis renders them non-productive, in contrast to MCMV, when despite the presence of IE1/IE3-GFP, the infected cells can progress through several cell cycles (Maul and Negorev, 2008).

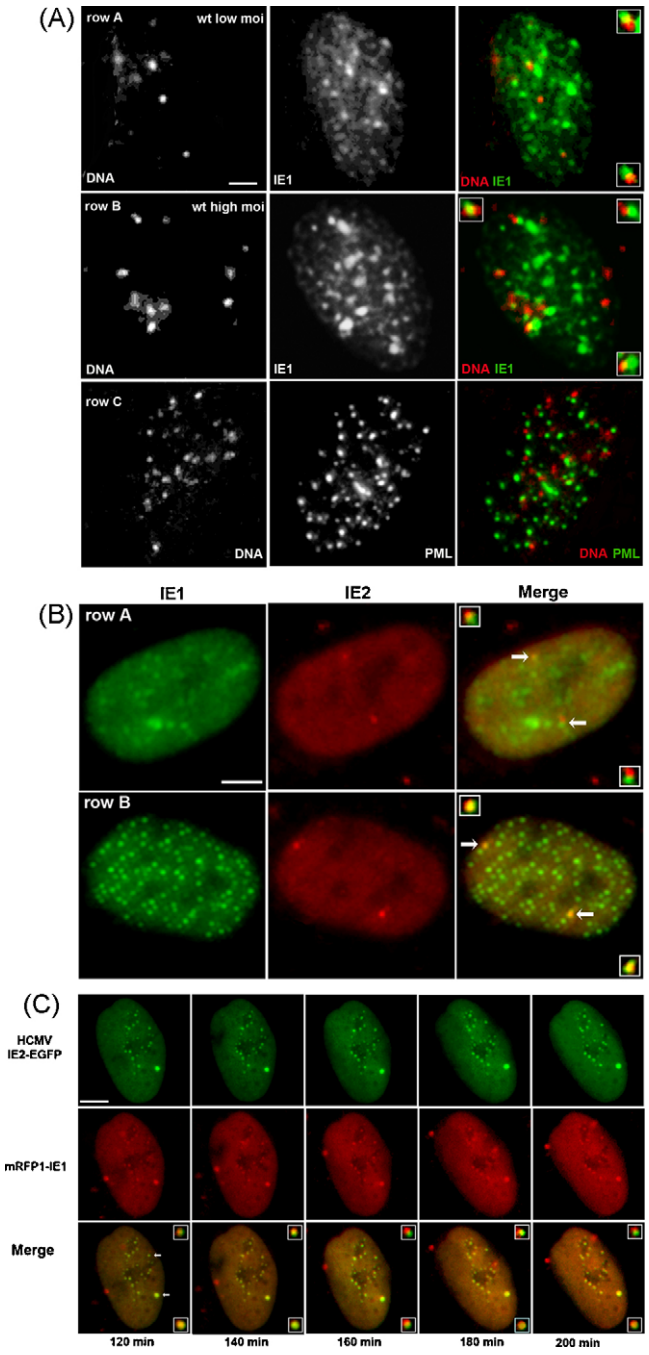

Fig. 3. Differential localization of IE1 with HCMV parental genomes and IE2 during the immediate early phase of infection. (A) Combined *in situ* hybridization of HCMV DNA and immunostaining of IE1 of CR401-infected HFFs, either at M.O.I. = 0.1 (row A) or M.O.I. = 1 (row B), demonstrated an association between the foci at 2.5 h p.i., analogous to association of viral DNA to ND10 (row C). (B) HHFs were infected with CR401 and stained for IE2 at early times post infection. All IE2 foci were either associated or partially co-localized with IE1 domains. The infection in row A has been terminated slightly later (4 h p.i.) than that in row B (3 h p.i.) and thus IE1 appears as punctate foci interspersed with diffuse staining. (C) *In vivo* dynamics of IE1 in relation to that of IE2. HFFs transfected with plasmid mRFP-IE1 were subsequently superinfected with HCMV AD169/IE2-EGFP at M.O.I. = 1 and monitored at early times. Selected images are presented, illustrating a dynamic pattern of association where, within minutes, IE1 and IE2 foci constantly change relative positions, interplaying between co-localization and juxtaposition. The inset images show regions of cells at higher magnification (bars, 10 μm). In all cases, images shown are representative of the population of cells observed in experiments.

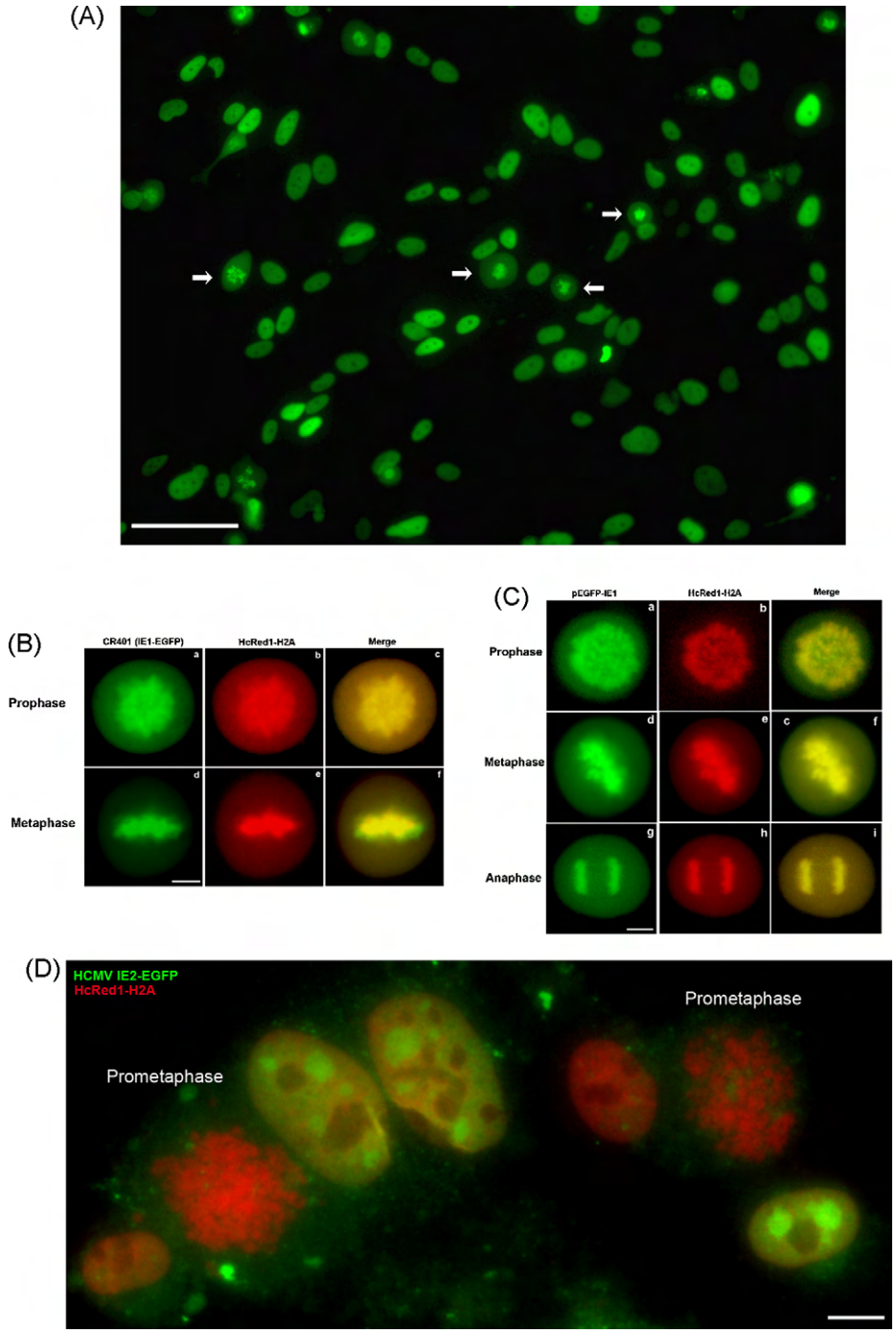

Fig. 4. Live-cell visualization of IE1 recruited onto metaphase chromatin. (A) Unsynchronized HFFs were infected with HCMV CR401 at M.O.I. = 1 and images were captured in live cells 72 h p.i. Arrows indicate the chromatin-associated localization of IE1 (bar, 10 μm). (B) IE1-EGFP fluorescence exhibits a labelling pattern identical to that of H2A throughout mitosis in CR401-infected fibroblasts expressing HcRed1-H2A. (C) HeLa cells were transiently co-transfected with pEGFP-IE1 and pHcRed1-H2A and monitored through mitosis. Live-cell imaging revealed that IE1 was clearly associated with condensed chromatin at various stages of cell division. (D) Localization of HCMV IE2 protein during mitosis. Normal fibroblasts were infected with HCMV AD169/IE2-EGFP at MOI = 1 and transfected with pHcRed1-H2A. In cells entering mitosis (second and sixth, left to right), IE2 was mainly diffuse in the nucleoplasm and not associated with metaphase chromatin. Note the well-formed viral replication compartments (third, fourth, seventh cell, left to right) as indicated by the recruitment of IE2 (72 h p.i.).

Since HCMV arrests cell cycle progression, the association of IE1-72K with metaphase chromatin is more readily followed in transfected cells (Nevels et al., 2004; Reinhardt et al., 2005). At the beginning of chromatin condensation, in prophase, H2A became associated with condensing chromosomes (Fig. 4C, b) while at the same mitotic phase, IE1-72K changed its initial diffuse nuclear localization to a condensed pattern which was identical to the H2A pattern (Fig. 4C, a). The intensive fluorescence of both IE1-72K and H2A associated with chromosomes became more evident in prometaphase and later on in metaphase (Fig. 4C, d–f). Remarkably, IE1-72K and H2A continued to co-migrate, being associated with mitotic chromosomes until the later stages of cell division (Fig. 4C, g–i). EGFP alone failed to bind to metaphase chromatin (not shown).

IE1 and IE2 share exons 1–3 (Fig. 1A), their encoded proteins both traffic to ND10 and exhibit a diffuse nuclear distribution

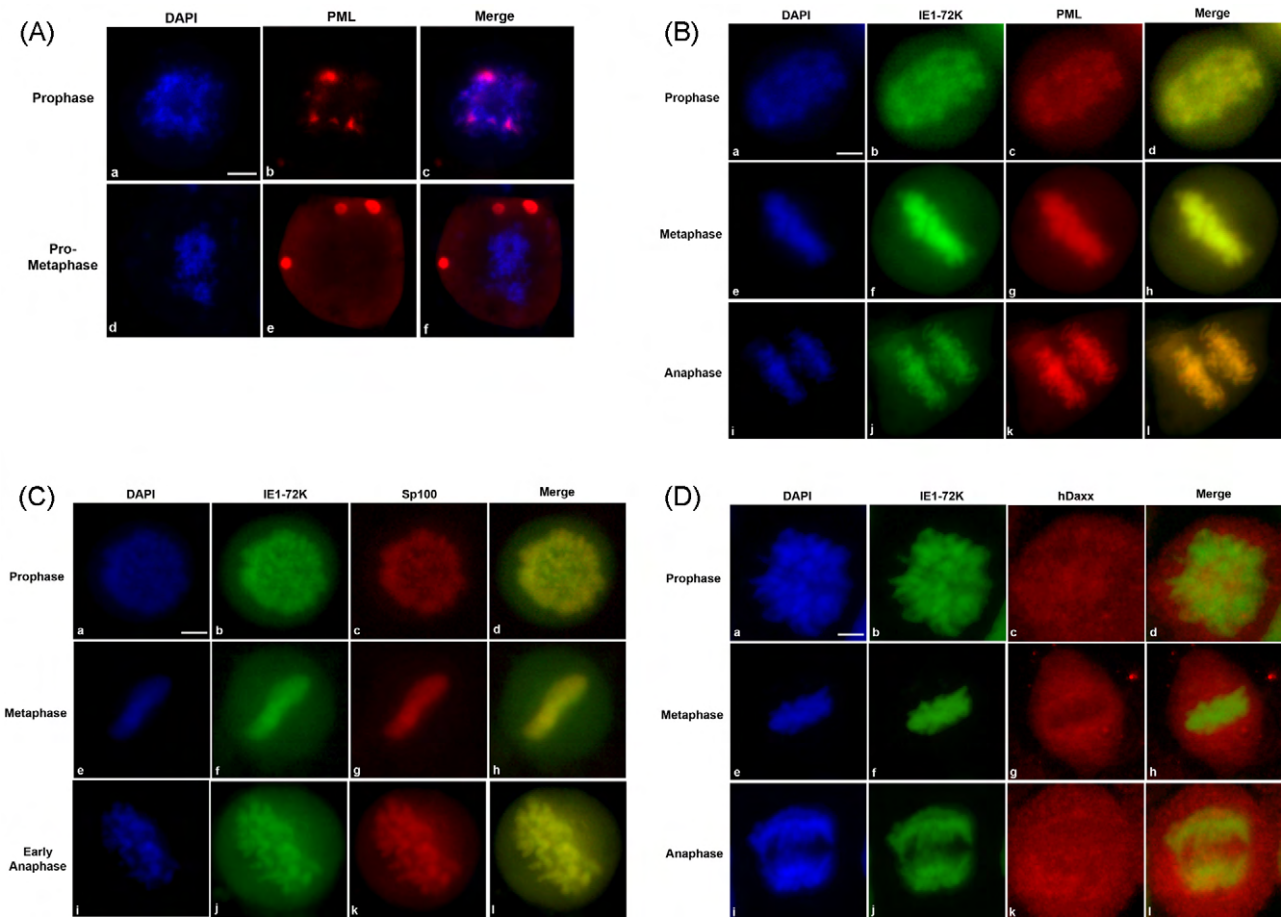

Fig. 5. IE1 recruits PML and Sp100 but not hDaxx onto condensed chromatin during mitosis in HCMV-infected cells. HFF cells were either mock infected (A) or infected with wild-type AD169 (B–D) and fixed 72 h p.i. The cells were immunostained for IE1-72K, PML, Sp100 and Daxx, followed by incubation with a mouse-specific Alexa Fluor 488 conjugate, a rabbit-specific Cy3 conjugate, and DAPI. (A) PML forms irregular accumulations in mitotic mock-infected cells. (B) The expression of IE1-72K drastically changes the localization of PML during mitosis, which becomes associated with condensed chromatin. (C). Sp100 is recruited onto metaphase chromatin when IE1-72K is expressed. (D). hDaxx remains diffuse during mitosis despite the presence of IE1-72K. Note the exclusion pattern of hDaxx, particularly during metaphase (g), from the space occupied by the condensed chromosomes (bars, 10 μm).

through the early/late phases of infection, However, IE2-GFP clearly does not bind to metaphase chromatin (Fig. 4D). Even during interphase, the IE2-86K and histone H2A staining patterns were distinct.

The above experiments demonstrate that there is an apparent differentiation regarding mitotic progression, depending on the mode of IE1-72K expression. Although IE1-transfected cells can readily be followed through mitosis, this is not the case in HCMV-infected cell cultures, where cells tend to persist in extended prophase or metaphase and infected cells are yet to be detected in anaphase.

IE1-72K recruits PML, Sp100 but not hDaxx to mitotic chromatin

We sought to investigate the association of ND10-associated proteins with metaphase chromatin in live cells and during productive virus infection. In uninfected cells lacking IE1-72K, PML foci persist through in mitosis with PML persisting as irregular accumulations that were excluded from condensed chromatin (Fig. 5A). In prophase, the number of such foci per cell was generally fewer than ND10 during interphase, and decreased even further in prometaphase; PML domains must either fuse or disassemble during this process. In metaphase and anaphase, brighter PML aggregates tended to be located adjacent to the metaphase plate (Fig. 5A, d–f). These distributions of PML were maintained throughout mitosis until the earliest stages of G1 (data not shown).

In wild-type HCMV-infected cells, IE1-72K and endogenous PML associated with mitotic chromatin (Fig. 5B). When cells entered prophase, the localization patterns of IE1-72K (Fig. 5B, b) and PML were identical (Fig. 5B, c); this indicates that a significant proportion of IE1-72K remained chromosome-bound as cells entered mitosis. Chromatin association of IE1-72K and PML endured throughout mitosis (Fig. 5B, f–l). Similar tethering of IE-72K and PML onto metaphase chromosomes was also observed in transient co-expression assays of EGFP-IE1 and ECFP-PML in live transfected cells (see Supplementary Fig. S4, B), confirming that this association is specific and not due to the presence of the fluorophore tags. Our observations demonstrate that expression of IE1-72K alone is sufficient to drive PML association with mitotic chromatin.

Sp100 was also found to associate with chromatin during cell division, either in wild-type HCMV-infected cells (Fig. 5C) or after co-expression of its fluorescent version mCherry-Sp100 with EGFP-IE1 by DNA transfection (see Supplementary Fig. S4, C). Both proteins labelled condensing chromosomes in prophase and remaining associated throughout mitosis. In contrast, endogenous hDaxx was excluded from the space occupied by the mitotic chromosomes in wild-type HCMV-infected cells (Fig. 5D, c, g, k). Similarly, diffuse localization of hDaxx was also observed in transient co-expression assays of either EGFP-IE1 and mCherry-hDaxx (see Supplementary Fig. S4, D) or even after the additional overexpression of ECFP-PML (data not shown). These results indicate

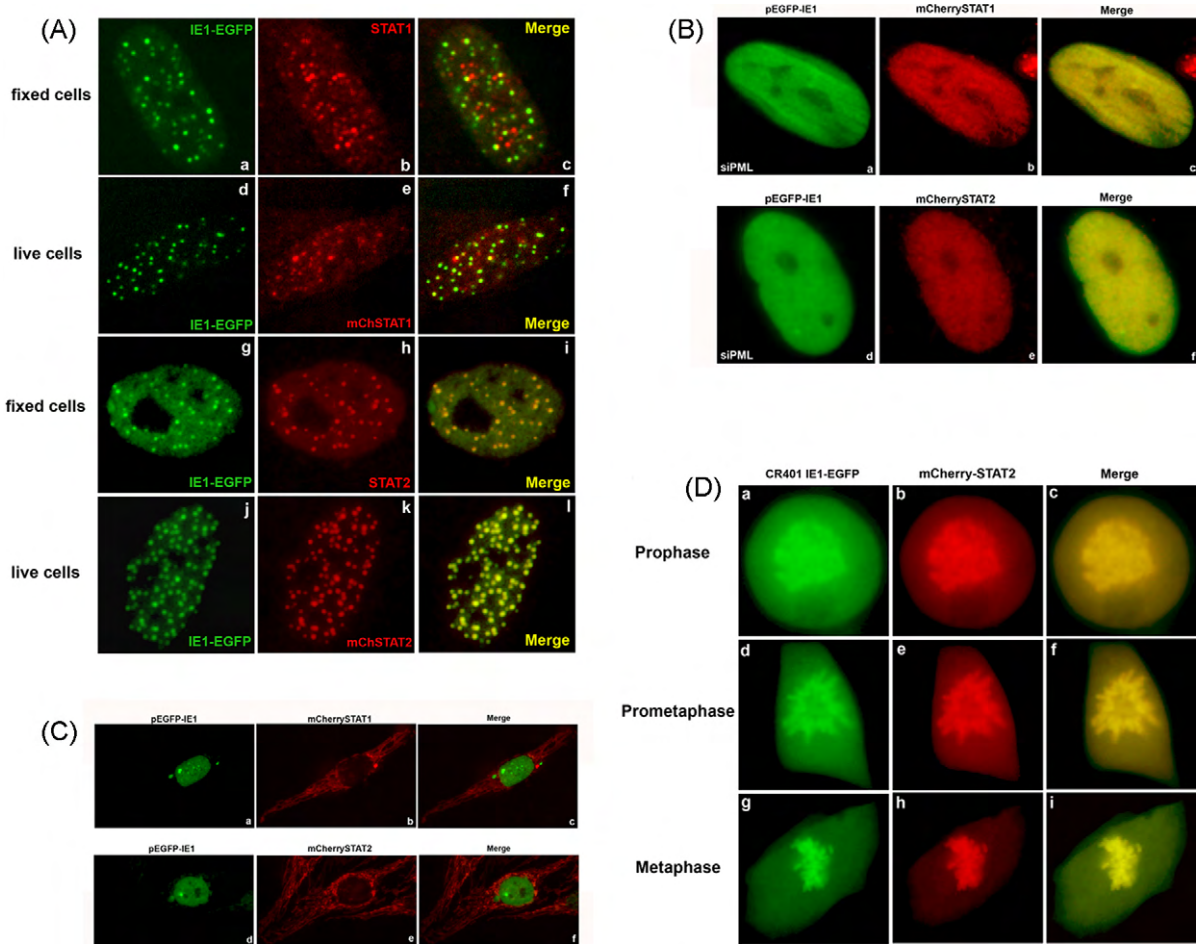

Fig. 6. IE1, STAT1 and STAT2 localization upon HCMV infection. (A) HFFs were infected with CR401 virus at M.O.I. = 1 and immunostained for STAT1 (a–c) and STAT2 (g–i) at 2–3 h p.i. Images from live cells were also captured after transfection of HFFs with mCherry-STAT1 (d–f) and mCherry-STAT2 (j–i) and subsequent superinfection with CR401 at M.O.I. = 1 for 2.5 h p.i. (B) Diffuse localization of IE1 and STAT1 (a–c) or STAT2 (d–f) in transiently transfected PML-kd cells. (C) STAT1/2 proteins are localized in separate cellular compartments in the absence of viral infection. HeLa cells were co-transfected with pEGFP-IE1 and either mCherry-STAT1 (a–c) or mCherry-STAT2 (d–f). (D) Images from live mitotic CR401-infected HFFs, expressing mCherry-STAT2, show the recruitment of IE1 and STAT2 onto condensed chromosomes at different stages of cell division (a–i).

IE1-72K may act to suppress the recognized interaction between PML and hDaxx so that during mitosis hDaxx fails to interact with PML or chromatin.

Spatial localization between HCMV IE1-72K, STAT1 and STAT2

IE1-72K inhibits the induction of type-1 interferon by formation of a physical complex with STAT1 and STAT2; furthermore STAT2 was shown by immunofluorescence to associate with mitotic chromatin in an IE1-expressing cell line (Krauss et al., 2009; Paulus et al., 2006). We therefore sought to investigate the spatial organization of STAT1 and STAT2 during productive infection by HCMV CR401. At early times of infection, both proteins translocated to the nucleus. While STAT1 migrated to foci in the nucleus, only a fraction co-localized with IE1-72K (Fig. 6A, a–c). In contrast, STAT2 co-localization with punctate forms of IE1-72K was comprehensive (Fig. 6A, g–i). Similar results were obtained with fixed and by live-cell imaging (Fig. 6A, d–f, j–i).

The function of IE1-72K was further tested in human fibroblasts with a stable siRNA knockdown of PML, termed PML-kd cells (Tavalai et al., 2006). In PML-kd cells infected with CR401, both IE1-72K and STAT1 or STAT2 were displaced into nuclear-diffuse forms (Fig. 6B), consistent with PML being required for the punctate distribution of IE1-72K and STAT2 at early times of infection. Virus infection or interferon induction was required to relocalize STAT-1 and STAT-2 from the cytoplasm to the nucleus; EGFP-IE1 expression alone was not sufficient. In transient expression studies, EGFP-IE1 trafficked to the nucleus while both mCherry-STAT1 or mCherry-STAT2 remained cytoplasmic (Fig. 6C).

STAT2 associates with condensed chromatin in fixed cells continuously expressing IE1-72K and treated with interferon (Paulus et al., 2006). We tracked mCherry-STAT2 in living cells following infection with HCMV CR401, where IE1-EGFP and mCherry-STAT2 clearly co-localized at ND10. Strikingly, in the small proportion of cells undergoing mitosis, both IE1-72K and STAT2 both labelled condensed chromosomes (Fig. 6D). The predominant targeting of IE1-72K and STAT2 to metaphase chromosomes was evident from the early stages of mitosis through to metaphase (Fig. 6D). Identical association between IE1-72K expressed by the wild-type HCMV and the endogenous STAT2 was also observed in fixed cells, confirming that the localization of the unlabelled proteins is not affected by the tags (see Supplementary Fig. S5). In contrast, STAT1 was excluded from mitotic chromatin even in the presence of IE1-72K (data not shown). These observations are consistent with a model in which HCMV infection induces activation of STAT2, but following transport of STAT2 to the nucleus it is sequestered by IE1-72K.

Discussion

The generation of recombinant viruses encoding both IE1-72K and IE2-86K EGFP fusion proteins now provides a robust technology to track expression from the HCMV major gene locus in real time. These viruses have widespread application in experimental models of virus latency/reactivation and evaluating antiviral compounds. In this study, we focussed primarily on IE1-72K interactions with ND10 component both during the very earliest stage (6 h) of HCMV productive infection, and in cells undergoing mitosis. Live-cell imaging avoids potential artefacts induced by cell fixation, while enabling gene expression, protein–protein interactions to be followed in time and space.

The growth properties of HCMV CR401 were characterized in detail prior to initiating imaging studies. While both the abundance and kinetics of IE1-72K-EGFP and IE2-86K expression were comparable with the parental virus strain, a modest reproducible growth defect was detected but only when infection was performed at an M.O.I. less than 1 PFU/cell. The structure and regulation of the major IE transcriptional unit is complex with multiple splice variants and early/late transcripts also being derived from this region (Meier and Stinski, 1996). Insertion of a substantial sequence element (EGFP) in this complex may be expected to have some impact on RNA processing (White and Spector, 2005). Fusion of EGFP to the C-terminus of *ie*1 could potentially impact on an IE1-72K function required for efficient replication.

Live-cell microscopy of HCMV CR401-infected cells imaged IE1-72K trafficking to ND10 by 2 h p.i. followed by the gradual yet comprehensive destruction of their integrity through to 6 h p.i.; during this process PML became desumolyated with similar kinetics compared to wild-type HCMV. The spatial organization of the parental genomes within the nucleus is a key element for the outcome of a viral infection. Our studies implicate IE1-72K in the formation of this nucleoprotein complex at very early times after infection (Fig. 3A). IE1 foci were positioned adjacent or partially co-localized with parental viral genomes in a mode reminiscent to the juxtaposition between HCMV parental genomes and ND10 (Ahn and Hayward, 1997; Ahn et al., 1999; Ishov et al., 1997; Sourvinos et al., 2007). The IE2-86K protein was also part of this viral nucleoprotein complex at early times of infection, although there were subtle differences between IE1-72K and IE2-86K localization. While these proteins are thought to act synergistically in the activation of transcription, our data indicates they are physically separated during infection, without any evidence of direct interaction, although both localize in the nucleus. Thus, from its earliest stages, virus infection must involve a structured assembly of viral proteins and DNA with respect to the cellular architecture, which is likely to be crucial for the progress of viral infection, common to the alpha- and beta-herpesviruses (Everett et al., 2003).

While PML persists in the nucleus after the ND10 disruption, Sp100 follows a distinct fate. When expressed in transient assays IE1-72K abrogates the covalent linkage of SUMO-1 to Sp100 and lower molecular-weight forms of Sp100 are retained (Muller and Dejean, 1999). The difficulties in visualizing the endogenous Sp100 preclude direct analysis of its spatial organization during an actual HCMV infection. The dispersal of Sp100, as observed by time-lapse microscopy, coupled with the loss of sumoylated-Sp100 revealed by the biochemical analysis at early times of HCMV infection, further corroborates the previously described destruction of ND10-like Sp100 accumulations which are transiently formed early after infection in the apparent absence of PML, in an IE1-72K-dependent manner (Tavalai et al., 2006). During mitosis, Sp100 is not physically associated with condensed chromatin but rapidly diffuses into the mitotic nucleoplasm (Dellaire et al., 2006). IE1-72K expression proves to be a strong mediator which dramatically alters the trafficking of Sp100 and results in the establishment of novel interactions with metaphase chromatin, favouring or inhibiting functions of Sp100.

Live-cell imaging using the CR401 virus reproduced the observation (in fixed cells) that IE1-72K associates strongly with STAT2 during productive infection, and weakly with STAT1 (Huh et al., 2008; Krauss et al., 2009; Paulus et al., 2006). HCMV binding and infection is recognized to induce a strong interferon response that is moderated by virus-encoded immune evasion functions (Browne and Shenk, 2003; Browne et al., 2001). Nuclear transport of STAT2 was IE1-72K-independent, and thus IE1-72K acts to sequester STAT2 post-activation. The IE1-72K/STAT2/PML/Sp100 complex appears stable, as it is manifested by their co-association with mitotic chromatin. Stable interactions with IE1-72K would appear to correlate with sequestration and loss of function.

The functional significance of the differential accumulation of ND10 components onto metaphase chromatin during mitosis upon IE1-72K expression remains to be addressed. Unlike an HCMV-infected, an IE1-72K-expressing cell line will go through mitosis. Thus, an association of IE1-72K, PML and/or Sp100 with chromatin is not causing the mitotic block, rather a unique and efficient biomarker that reveals IE1-72K sequesters these functions en bloc. We believe an independent HCMV gene to be responsible, but its identification it is not trivial. We propose that IE1-72K takes PML, Sp100 and STAT-2 to cellular chromatin to sequester their function. We consider this an important event however, the reason for the association with chromatin is not clear. The association with chromatin *per se* is not 'crucial' as an HCMV IE1 mutant with a deletion in the chromatin-binding domain has no overt growth defect in fibroblasts *in vitro* (Reinhardt et al., 2005; Wilkinson et al., 1998). However, the effect may manifest in different cell type or *in vivo*. As regards STAT-2, the study in the context of a productive HCMV infection is particularly informative, as we have shown that HCMV both induces and sequesters the STAT-2 function. STAT1 acts in combination with STAT-2, thus their physical dissociation is clearly important. Although HCMV can replicate in the absence of IE1-72K, so the effect is not essential for virus propagation *in vitro* however, the situation is likely to be different *in vivo*.

hDaxx was identified through its cytoplasmic interaction with Fas, and is pro-apototic following stimulation. hDaxx is also constitutively present in the nucleus where it associates with ND10, and acts to suppress HCMV IE gene expression (Cantrell and Bresnahan, 2006; Preston and Nicholl, 2006; Saffert and Kalejta, 2006; Woodhall et al., 2006). The HCMV tegument protein pp71 promotes proteosome-mediated degradation of hDaxx, and thereby relieves hDaxx-mediated repression of IE gene expression (Saffert and Kalejta, 2006). hDaxx naturally accumulates at the condensed heterochromatic areas in late S phase (Ishov et al., 1999), but not with metaphase chromatin (Pluta et al., 1998). The recognized interaction between hDaxx and PML is dependent on sumoylation (Ishov et al., 1999; Li et al., 2000), thus IE1-mediated desumolyation of PML can be expected to dissociate this complex during HCMV infection. The fact that PML, and not hDaxx is tethered by IE1-72K to metaphase chromatin, is consistent with the hDaxx-PML being dissociated during infection. The release of hDaxx to the cytoplasm, suggests that it is sufficient to break the association with PML/ND10 to relieve hDaxx-mediated suppression of HCMV infection. While the association of hDaxx with PML is pro-apoptotic, there is evidence that hDaxx may be anti-apoptotic properties when is free of PML (Chen and Chen, 2003). By releasing hDaxx to the nucleoplasm free from its complex with PML, IE1 may selectively modulate the function of hDaxx.

The C-terminus of IE1-72K is required for the interaction with chromatin, but for neither ND10 disruption (Wilkinson et al., 1998) nor productive virus replication *in vitro* (Reinhardt et al., 2005). Thus, the significance of this interaction with higher-order structures of the host cell nucleus remains uncertain. It remains to be

determined if there is any functional significance in the differential accumulation of ND10 components on to metaphase chromatin by IE1-72K expression. IE1-72K tethering to condensed chromatin was readily detectable in transiently transfected cells, where IE expression is fully compatible with cell cycle progression. While HCMV is recognized to promote cell cycle arrest, this is thought to occur under conditions approximating to late G1/S phase (Bresnahan et al., 1996; Jault et al., 1995). Nevertheless, mitotic cells were readily detected by IE1-EGFP chromatin staining in a population of HCMV CR401-infected cells. This observation is consistent with data from FACS analysis, showing that a very small population of the cells that are infected while the cells are actively replicating their DNA are able to express the IE proteins in the G2/M phase of the cell cycle (Fortunato et al., 2002). However, when followed by live-cell imaging, these cells failed to progress out of metaphase through cell division. An HCMV gene function(s), which is not IE1-72K, appears to impose a blockade on cell mitosis.

Acknowledgments

We thank Drs. B. Plachter (Mainz, Germany) and N. Kretsovali (Crete, Greece) for providing reagents. This work was supported by a Marie Curie Reintegration Grant of the European Commission Framework 6 Programme (contract no. MERG-CT-2004-513448). Jonathan Gawn, Emma Sherratt, Carole Rickards and Marian Denson contributed to preliminary studies characterizing the HCMV IE1-EGFP recombinant. GW, RC and BMcS were supported by funding from the Wellcome Trust, BBSRC, and Medical Research Council (UK). PD received funding from Erasmus.

Appendix A. Supplementary data

Supplementary data associated with this article can be found, in the online version, at doi:10.1016/j.ejcb.2010.05.006.

References

Ahn, J.H., Brignole 3rd, E.J., Hayward, G.S., 1998. Disruption of PML subnuclear domains by the acidic IE1 protein of human cytomegalovirus is mediated through interaction with PML and may modulate a RING finger-dependent cryptic transactivator function of PML. Mol. Cell. Biol. 18, 4899–4913.

Ahn, J.H., Hayward, G.S., 1997. The major immediate-early proteins IE1 and IE2 of human cytomegalovirus colocalize with and disrupt PML-associated nuclear bodies at very early times in infected permissive cells. J. Virol. 71, 4599–4613.

Ahn, J.H., Jang, W.J., Hayward, G.S., 1999. The human cytomegalovirus IE2 and UL112-113 proteins accumulate in viral DNA replication compartments that initiate from the periphery of promyelocytic leukemia protein-associated nuclear bodies (PODs or ND10). J. Virol. 73, 10458–10471.

Ahn, K., Angulo, A., Ghazal, P., Peterson, P.A., Yang, Y., Fruh, K., 1996. Human cytomegalovirus inhibits antigen presentation by a sequential multistep process. Proc. Natl. Acad. Sci. U.S.A. 93, 10990–10995.

Andreoni, M., Faircloth, M., Vugler, L., Britt, W.J., 1989. A rapid microneutralization assay for the measurement of neutralizing antibody reactive with human cytomegalovirus. J. Virol. Methods 23, 157–167.

Bernardi, R., Pandolfi, P.P., 2003. Role of PML and the PML-nuclear body in the control of programmed cell death. Oncogene 22, 9048–9057.

Borst, E.M., Hahn, G., Koszinowski, U.H., Messerle, M., 1999. Cloning of the human cytomegalovirus (HCMV) genome as an infectious bacterial artificial chromosome in Escherichia coli: a new approach for construction of HCMV mutants. J. Virol. 73, 8320–8329.

Boyle, K.A., Pietropaolo, R.L., Compton, T., 1999. Engagement of the cellular receptor for glycoprotein B of human cytomegalovirus activates the interferon-responsive pathway. Mol. Cell. Biol. 19, 3607–3613.

Bresnahan, W.A., Boldogh, I., Thompson, E.A., Albrecht, T., 1996. Human cytomegalovirus inhibits cellular DNA synthesis and arrests productively infected cells in late G1. Virology 224, 150–160.

Browne, E.P., Shenk, T., 2003. Human cytomegalovirus UL83-coded pp65 virion protein inhibits antiviral gene expression in infected cells. Proc. Natl. Acad. Sci. U.S.A. 100, 11439–11444.

Browne, E.P., Wing, B., Coleman, D., Shenk, T., 2001. Altered cellular mRNA levels in human cytomegalovirus-infected fibroblasts: viral block to the accumulation of antiviral mRNAs. J. Virol. 75, 12319–12330.

Cantrell, S.R., Bresnahan, W.A., 2006. Human cytomegalovirus (HCMV) UL82 gene product (pp71) relieves hDaxx-mediated repression of HCMV replication. J. Virol. 80, 6188–6191.

Castillo, J.P., Yurochko, A.D., Kowalik, T.F., 2000. Role of human cytomegalovirus immediate-early proteins in cell growth control. J. Virol. 74, 8028–8037.

Caswell, R., Hagemeier, C., Chiou, C.J., Hayward, G., Kouzarides, T., Sinclair, J., 1993. The human cytomegalovirus 86K immediate early (IE) 2 protein requires the basic region of the TATA-box binding protein (TBP) for binding, and interacts with TBP and transcription factor TFIIB via regions of IE2 required for transcriptional regulation. J. Gen. Virol. 74 (Pt 12), 2691–2698.

Chen, L.Y., Chen, J.D., 2003. Daxx silencing sensitizes cells to multiple apoptotic pathways. Mol. Cell. Biol. 23, 7108–7121.

Cherrington, J.M., Mocarski, E.S., 1989. Human cytomegalovirus ie1 transactivates the alpha promoter-enhancer via an 18-base-pair repeat element. J. Virol. 63, 1435–1440.

Child, S.J., Hakki, M., De Niro, K.L., Geballe, A.P., 2004. Evasion of cellular antiviral responses by human cytomegalovirus TRS1 and IRS1. J. Virol. 78, 197–205.

Choi, Y.H., Bernardi, R., Pandolfi, P.P., Benveniste, E.N., 2006. The promyelocytic leukemia protein functions as a negative regulator of IFN-gamma signaling. Proc. Natl. Acad. Sci. U.S.A. 103, 18715–18720.

Dellaire, G., Bazett-Jones, D.P., 2004. PML nuclear bodies: dynamic sensors of DNA damage and cellular stress. Bioassays 26, 963–977.

Dellaire, G., Eskiw, C.H., Dehghani, H., Ching, R.W., Bazett-Jones, D.P., 2006. Mitotic accumulations of PML protein contribute to the re-establishment of PML nuclear bodies in G1. J. Cell Sci. 119, 1034–1042.

Everett, R.D., 2006. Interactions between DNA viruses, ND10 and the DNA damage response. Cell. Microbiol. 8, 365–374.

Everett, R.D., Murray, J., 2005. ND10 components relocate to sites associated with herpes simplex virus type 1 nucleoprotein complexes during virus infection. J. Virol. 79, 5078–5089.

Everett, R.D., Sourvinos, G., Orr, A., 2003. Recruitment of herpes simplex virus type 1 transcriptional regulatory protein ICP4 into foci juxtaposed to ND10 in live, infected cells. J. Virol. 77, 3680–3689.

Fortunato, E.A., Sanchez, V., Yen, J.Y., Spector, D.H., 2002. Infection of cells with human cytomegalovirus during S phase results in a blockade to immediate-early gene expression that can be overcome by inhibition of the proteasome. J. Virol. 76, 5369–5379.

Gawn, J.M., Greaves, R.F., 2002. Absence of IE1 p72 protein function during low-multiplicity infection by human cytomegalovirus results in a broad block to viral delayed-early gene expression. J. Virol. 76, 4441–4455.

Goldmacher, V.S., Bartle, L.M., Skaletskaya, A., Dionne, C.A., Kedersha, N.L., Vater, C.A., Han, J.W., Lutz, R.J., Watanabe, S., Cahir McFarland, E.D., Kieff, E.D., Mocarski, E.S., Chittenden, T., 1999. A cytomegalovirus-encoded mitochondria-localized inhibitor of apoptosis structurally unrelated to Bcl-2. Proc. Natl. Acad. Sci. U.S.A. 96, 12536–12541.

Greaves, R.F., Mocarski, E.S., 1998. Defective growth correlates with reduced accumulation of a viral DNA replication protein after low-multiplicity infection by a human cytomegalovirus ie1 mutant. J. Virol. 72, 366–379.

Huh, Y.H., Kim, Y.E., Kim, E.T., Park, J.J., Song, M.J., Zhu, H., Hayward, G.S., Ahn, J.H., 2008. Binding STAT2 by the acidic domain of human cytomegalovirus IE1 promotes viral growth and is negatively regulated by SUMO. J. Virol. 82, 10444–10454.

Ishov, A.M., Maul, G.G., 1996. The periphery of nuclear domain 10 (ND10) as site of DNA virus deposition. J. Cell Biol. 134, 815–826.

Ishov, A.M., Sotnikov, A.G., Negorev, D., Vladimirova, O.V., Neff, N., Kamitani, T., Yeh, E.T., Strauss 3rd, J.F., Maul, G.G., 1999. PML is critical for ND10 formation and recruits the PML-interacting protein daxx to this nuclear structure when modified by SUMO-1. J. Cell Biol. 147, 221–234.

Ishov, A.M., Stenberg, R.M., Maul, G.G., 1997. Human cytomegalovirus immediate early interaction with host nuclear structures: definition of an immediate transcript environment. J. Cell Biol. 138, 5–16.

Ishov, A.M., Vladimirova, O.V., Maul, G.G., 2004. Heterochromatin and ND10 are cell-cycle regulated and phosphorylation-dependent alternate nuclear sites of the transcription repressor Daxx and SWI/SNF protein ATRX. J. Cell Sci. 117, 3807–3820.

Jault, F.M., Jault, J.M., Ruchti, F., Fortunato, E.A., Clark, C., Corbeil, J., Richman, D.D., Spector, D.H., 1995. Cytomegalovirus infection induces high levels of cyclins, phosphorylated Rb, and p53, leading to cell cycle arrest. J. Virol. 69, 6697–6704.

Kelly, C., Van Driel, R., Wilkinson, G.W., 1995. Disruption of PML-associated nuclear bodies during human cytomegalovirus infection. J. Gen. Virol. 76 (Pt 11), 2887–2893.

Korioth, F., Maul, G.G., Plachter, B., Stamminger, T., Frey, J., 1996. The nuclear domain 10 (ND10) is disrupted by the human cytomegalovirus gene product IE1. Exp. Cell Res. 229, 155–158.

Krauss, S., Kaps, J., Czech, N., Paulus, C., Nevels, M., 2009. Physical requirements and functional consequences of complex formation between the cytomegalovirus IE1 protein and human STAT2. J. Virol. 83, 12854–12870.

Lafemina, R.L., Pizzorno, M.C., Mosca, J.D., Hayward, G.S., 1989. Expression of the acidic nuclear immediate-early protein (IE1) of human cytomegalovirus in stable cell lines and its preferential association with metaphase chromosomes. Virology 172, 584–600.

Lalioti, M., Heath, J., 2001. A new method for generating point mutations in bacterial artificial chromosomes by homologous recombination in Escherichia coli. Nucleic Acids Res. 29, pE14.

Lee, H.R., Kim, D.J., Lee, J.M., Choi, C.Y., Ahn, B.Y., Hayward, G.S., Ahn, J.H., 2004. Ability of the human cytomegalovirus IE1 protein to modulate sumoylation of PML correlates with its functional activities in transcriptional regulation and infectivity in cultured fibroblast cells. J. Virol. 78, 6527–6542.

Li, H., Leo, C., Zhu, J., Wu, X., O'Neil, J., Park, E.J., Chen, J.D., 2000. Sequestration and inhibition of Daxx-mediated transcriptional repression by PML. Mol. Cell. Biol. 20, 1784–1796.

Lukashchuk, V., McFarlane, S., Everett, R.D., Preston, C.M., 2008. Human cytomegalovirus protein pp71 displaces the chromatin-associated factor ATRX from nuclear domain 10 at early stages of infection. J. Virol. 82, 12543–12554.

Malone, C.L., Vesole, D.H., Stinski, M.F., 1990. Transactivation of a human cytomegalovirus early promoter by gene products from the immediate-early gene IE2 and augmentation by IE1: mutational analysis of the viral proteins. J. Virol. 64, 1498–1506.

Marchini, A., Liu, H., Zhu, H., 2001. Human cytomegalovirus with IE-2 (UL122) deleted fails to express early lytic genes. J. Virol. 75, 1870–1878.

Maul, G.G., Ishov, A.M., Everett, R.D., 1996. Nuclear domain 10 as preexisting potential replication start sites of herpes simplex virus type-1. Virology 217, 67–75.

Maul, G.G., Negorev, D., 2008. Differences between mouse and human cytomegalovirus interactions with their respective hosts at immediate early times of the replication cycle. Med. Microbiol. Immunol. 197, 241–249.

Meier, J.L., Stinski, M.F., 1996. Regulation of human cytomegalovirus immediate-early gene expression. Intervirology 39, 331–342.

Milovic-Holm, K., Krieghoff, E., Jensen, K., Will, H., Hofmann, T.G., 2007. FLASH links the CD95 signaling pathway to the cell nucleus and nuclear bodies. EMBOJ 26, 391–401.

Mocarski, E.S., Kemble, G.W., Lyle, J.M., Greaves, R.F., 1996. A deletion mutant in the human cytomegalovirus gene encoding IE1(491aa) is replication defective due to a failure in autoregulation. Proc. Natl. Acad. Sci. U.S.A. 93, 11321–11326.

Muller, S., Dejean, A., 1999. Viral immediate-early proteins abrogate the modification by SUMO-1 of PML and Sp100 proteins, correlating with nuclear body disruption. J. Virol. 73, 5137–5143.

Navarro, L., Mowen, K., Rodems, S., Weaver, B., Reich, N., Spector, D., David, M., 1998. Cytomegalovirus activates interferon immediate-early response gene expression and an interferon regulatory factor 3-containing interferon-stimulated response element-binding complex. Mol. Cell. Biol. 18, 3796–3802.

Negorev, D., Maul, G.G., 2001. Cellular proteins localized at and interacting within ND10/PML nuclear bodies/PODs suggest functions of a nuclear depot. Oncogene 20, 7234–7242.

Negorev, D.G., Vladimirova, O.V., Ivanov, A., Rauscher 3rd, F., Maul, G.G., 2006. Differential role of Sp100 isoforms in interferon-mediated repression of herpes simplex virus type 1 immediate-early protein expression. J. Virol. 80, 8019–8029.

Nevels, M., Brune, W., Shenk, T., 2004. SUMOylation of the human cytomegalovirus 72-kilodalton IE1 protein facilitates expression of the 86-kilodalton IE2 protein and promotes viral replication. J. Virol. 78, 7803–7812.

Pajovic, S., Wong, E.L., Black, A.R., Azizkhan, J.C., 1997. Identification of a viral kinase that phosphorylates specific E2Fs and pocket proteins. Mol. Cell. Biol. 17, 6459–6464.

Paulus, C., Krauss, S., Nevels, M., 2006. A human cytomegalovirus antagonist of type I IFN-dependent signal transducer and activator of transcription signaling. Proc. Natl. Acad. Sci. U.S.A. 103, 3840–3845.

Pizzorno, M.C., O'Hare, P., Sha, L., LaFemina, R.L., Hayward, G.S., 1988. Transactivation and autoregulation of gene expression by the immediate-early region 2 gene products of human cytomegalovirus. J. Virol. 62, 1167–1179.

Plachter, B., Britt, W., Vornhagen, R., Stamminger, T., Jahn, G., 1993. Analysis of proteins encoded by IE regions 1 and 2 of human cytomegalovirus using monoclonal antibodies generated against recombinant antigens. Virology 193, 642–652.

Pluta, A.F., Earnshaw, W.C., Goldberg, I.G., 1998. Interphase-specific association of intrinsic centromere protein CENP-C with HDaxx, a death domain-binding protein implicated in Fas-mediated cell death. J. Cell Sci. 111 (Pt 14), 2029–2041.

Preston, C.M., Nicholl, M.J., 2006. Role of the cellular protein hDaxx in human cytomegalovirus immediate-early gene expression. J. Gen. Virol. 87, 1113–1121.

Reboredo, M., Greaves, R.F., Hahn, G., 2004. Human cytomegalovirus proteins encoded by UL37 exon 1 protect infected fibroblasts against virus-induced apoptosis and are required for efficient virus replication. J. Gen. Virol. 85, 3555–3567.

Reeves, M., Murphy, J., Greaves, R., Fairley, J., Brehm, A., Sinclair, J., 2006. Autorepression of the human cytomegalovirus major immediate-early promoter/enhancer at late times of infection is mediated by the recruitment of chromatin remodeling enzymes by IE86. J. Virol. 80, 9998–10009.

Reinhardt, J., Smith, G.B., Himmelheber, C.T., Azizkhan-Clifford, J., Mocarski, E.S., 2005. The carboxyl-terminal region of human cytomegalovirus IE1491aa contains an acidic domain that plays a regulatory role and a chromatin-tethering domain that is dispensable during viral replication. J. Virol. 79, 225–233.

Saffert, R.T., Kalejta, R.F., 2006. Inactivating a cellular intrinsic immune defense mediated by Daxx is the mechanism through which the human cytomegalovirus pp71 protein stimulates viral immediate-early gene expression. J. Virol. 80, 3863–3871.

Simmen, K.A., Singh, J., Luukkonen, B.G., Lopper, M., Bittner, A., Miller, N.E., Jackson, M.R., Compton, T., Fruh, K., 2001. Global modulation of cellular transcription by human cytomegalovirus is initiated by viral glycoprotein B. Proc. Natl. Acad. Sci. U.S.A. 98, 7140–7145.

Sinzger, C., Grefte, A., Plachter, B., Gouw, A.S., The, T.H., Jahn, G., 1995. Fibroblasts, epithelial cells, endothelial cells and smooth muscle cells are major targets of human cytomegalovirus infection in lung and gastrointestinal tissues. J. Gen. Virol. 76 (Pt 4), 741–750.

Skaletskaya, A., Bartle, L.M., Chittenden, T., McCormick, A.L., Mocarski, E.S., Goldmacher, V.S., 2001. A cytomegalovirus-encoded inhibitor of apoptosis that suppresses caspase-8 activation. Proc. Natl. Acad. Sci. U.S.A. 98, 7829–7834.

Sourvinos, G., Everett, R.D., 2002. Visualization of parental HSV-1 genomes and replication compartments in association with ND10 in live infected cells. EMBOJ 21, 4989–4997.

Sourvinos, G., Tavalai, N., Berndt, A., Spandidos, D.A., Stamminger, T., 2007. Recruitment of human cytomegalovirus immediate-early 2 protein onto parental viral genomes in association with ND10 in live-infected cells. J. Virol. 81, 10123–10136.

Stanton, R.J., McSharry, B.P., Armstrong, M., Tomasec, P., Wilkinson, G.W., 2008. Re-engineering adenovirus vector systems to enable high-throughput analyses of gene function. Biotechniques 45, 659–662, 664–668.

Tang, J., Wu, S., Liu, H., Stratt, R., Barak, O.G., Shiekhattar, R., Picketts, D.J., Yang, X., 2004. A novel transcription regulatory complex containing death domain-associated protein and the ATR-X syndrome protein. J. Biol. Chem. 279, 20369–20377.

Tavalai, N., Papior, P., Rechter, S., Leis, M., Stamminger, T., 2006. Evidence for a role of the cellular ND10 protein PML in mediating intrinsic immunity against human cytomegalovirus infections. J. Virol. 80, 8006–8018.

Tavalai, N., Papior, P., Rechter, S., Stamminger, T., 2008. Nuclear domain 10 components promyelocytic leukemia protein and hDaxx independently contribute to an intrinsic antiviral defense against human cytomegalovirus infection. J. Virol. 82, 126–137.

White, E.A., Spector, D.H., 2005. Exon 3 of the human cytomegalovirus major immediate-early region is required for efficient viral gene expression and for cellular cyclin modulation. J. Virol. 79, 7438–7452.

Wilkinson, G.W., Kelly, C., Sinclair, J.H., Rickards, C., 1998. Disruption of PML-associated nuclear bodies mediated by the human cytomegalovirus major immediate early gene product. J. Gen. Virol. 79 (Pt 5), 1233–1245.

Woodhall, D.L., Groves, I.J., Reeves, M.B., Wilkinson, G., Sinclair, J.H., 2006. Human Daxx-mediated repression of human cytomegalovirus gene expression correlates with a repressive chromatin structure around the major immediate early promoter. J. Biol. Chem. 281, 37652–37660.

Zhu, H., Cong, J.P., Shenk, T., 1997. Use of differential display analysis to assess the effect of human cytomegalovirus infection on the accumulation of cellular RNAs: induction of interferon-responsive RNAs. Proc. Natl. Acad. Sci. U.S.A. 94, 13985–13990.